Deuteron Nuclear Magnetic Resonance Study of the Dynamic Organization of Phospholipid/Cholesterol Bilayer Membranes: Molecular Properties and Viscoelastic Behavior†

K. Weisz,‡ G. Gröbner, C. Mayer, J. Stohrer, and G. Kothe*

Institut für Physikalische Chemie, Universität Stuttgart, Pfaffenwaldring 55, D-7000 Stuttgart 80, Federal Republic of Germany

Received July 16, 1991; Revised Manuscript Received October 17, 1991

ABSTRACT: The influence of cholesterol on the dynamic organization of 1,2-dimyristoyl-*sn*-glycero-3-phosphocholine (DMPC) bilayers was studied by deuteron nuclear magnetic resonance (^{2}H NMR) using unoriented and macroscopically aligned samples. Analysis of the various temperature- and orientation-dependent experiments was performed using a comprehensive NMR model based on the stochastic Liouville equation. Computer simulations of the relaxation data obtained from phospholipids deuterated at the 6-, 13- and 14-position of the *sn*-2 chain and cholesterol labeled at the 3α-position of the rigid steroid ring system allowed the unambiguous assignment of the various motional modes and types of molecular order present in the system. Above the phospholipid gel-to-liquid-crystalline phase transition, T_M, 40 mol % cholesterol was found to significantly increase the orientational and conformational order of the phospholipid with substantially increased trans populations even at the terminal *sn*-2 acyl chain segments. Lowering the temperature continuously increases both inter- and intramolecular ordering, yet indicates less ordered chains than found for the pure phospholipid in its paracrystalline gel phase. Trans–gauche isomerization rates on all phospholipid alkyl chain segments are slowed down by incorporated cholesterol to values characteristic of gel-state lipid. However, intermolecular dynamics remain fast on the NMR time scale up to 30 K below T_M, with rotational correlation times $\tau_{R\parallel}$ for DMPC ranging from 10 to 100 ns and an activation energy of E_R = 35 kJ/mol. Below 273 K a continuous noncooperative condensation of both phospholipid and cholesterol is observed in the mixed membranes, and at about 253 K only a motionally restricted component is left, exhibiting slow fluctuations with correlation times of $\tau_{R\perp} > 1$ μs. In the high-temperature region ($T > T_M$), order director fluctuations are found to constitute the dominant transverse relaxation process. Analysis of these collective lipid motions provides the viscoelastic parameters of the membranes. The results (T = 318 K) show that cholesterol significantly reduces the density of the cooperative motions by increasing the average elastic constant of the membrane from $K = 1 \times 10^{-11}$ N for the pure phospholipid bilayers to $K = 3.5 \times 10^{-11}$ N for the mixed system.

Cholesterol is a major component in mammalian tissue and amounts up to 50 mol % of the total lipid in erythrocyte and myelin membranes. Its widespread occurrence and involvement in physiological malfunctions has stimulated the study of its structural and functional role in biological and model membranes by a variety of physical techniques. Among these are nuclear magnetic resonance (NMR)[1] (Gally et al., 1976; Stockton & Smith, 1976; Haberkorn et al., 1977; Oldfield et al., 1978), electron paramagnetic resonance (EPR) (Oldfield & Chapman, 1971; Schreier-Murillo et al., 1973; Taylor & Smith, 1980), fluorescence polarization (Fahey & Webb, 1978; Alecio et al., 1982), X-ray diffraction (Ladbrooke et al., 1968; McIntosh, 1978), and differential scanning calorimetry (DSC) (Estep et al., 1978; Mabrey et al., 1978). In some cases partial phase diagrams for binary phospholipid/cholesterol bilayers have been established based on the experimental data (Shimshick & McConnell, 1973; Vist & Davis, 1990).

Cholesterol is known to induce an overall ordering for phospholipid in the liquid-crystalline (L_α) phase, often referred to as the condensing effect of cholesterol, while disordering gel (L_β') phase lipid. Small amounts of the steroid are sufficient to completely suppress the pretransition from the paracrystalline (L_β') to the intermediate (P_β') phase for phosphatidylcholine dispersions, and increasing the cholesterol concentration leads to a broadening and subsequent elimination of the phospholipid gel-to-liquid-crystalline phase transition (T_M). However, despite the considerable knowledge already obtained about cholesterol and its influence on lipid membranes, the detailed molecular organization in phospholipid/cholesterol bilayers is far from being understood. This is particularly true for the complex dynamics in these systems with molecular motions covering a broad dynamic range. Much of the previous work on lipid dynamics in the membranes has been focused on fast molecular reorientations with frequencies above 10^6 Hz. In contrast, the characterization

† Financial support by Deutsche Forschungsgemeinschaft and Fonds der Chemischen Industrie is gratefully acknowledged.

* To whom correspondence should be addressed.

‡ Present address: UCSF Magnetic Resonance Laboratory, Department of Pharmaceutical Chemistry, The University of California, 926 Medical Science, San Francisco, CA 94143

[1] Abbreviations: NMR, nuclear magnetic resonance; EPR, electron paramagnetic resonance; DSC, differential scanning calorimetry; L_α phase, liquid-crystalline phase; P_β' phase, intermediate phase; L_β' phase, gel phase; T_M, gel-to-liquid-crystalline phase transition; CP pulse, composite pulse; CPMG, Carr–Purcell–Meiboom–Gill; DMPC, 1,2-dimyristoyl-*sn*-glycero-3-phosphocholine; 2-[*6,6-d*$_2$]DMPC, 1-myristoyl-2-(myristoyl-*6,6-d*$_2$)-*sn*-glycero-3-phosphocholine; 2-[*13,13-d*$_2$]DMPC, 1-myristoyl-2-(myristoyl-*13,13-d*$_2$)-*sn*-glycero-3-phosphocholine; 2-[*14,14,14-d*$_3$]DMPC, 1-myristoyl-2-(myristoyl-*14,14,14-d*$_3$)-*sn*-glycero-3-phosphocholine.

0006-2960/92/0431-1100$03.00/0

of low-frequency motional modes and their modulation by different membrane components has only recently become an important area of interest. Slow molecular fluctuations are thought to play a crucial role in many membrane functions such as ion and energy transport, enzymatic activity of proteins, and transmembrane signaling. Indeed, NMR studies indicated large changes in slow motional contributions upon cholesterol and protein addition to lipid bilayers (Cornell et al., 1982, 1983), thus corroborating the importance of low-frequency motions in lipid/cholesterol and lipid/protein interactions.

Pulsed dynamic NMR has long been established as a powerful tool for studying complex chemical and biological systems. The use of different pulse sequences allows detection of the motions over an extremely wide dynamic range not accessible by any other technique. Furthermore, variation of the magnetic field orientation provides additional information on the molecular dynamics, thus facilitating the discrimination of the various motional modes. We report here on a ^{2}H NMR relaxation study using specifically deuterated 1,2-dimyristoyl-*sn*-glycero-3-phosphocholine (DMPC) and cholesterol in fully hydrated bilayers. Analysis of the relaxation experiments is performed using a comprehensive NMR model which is valid in both fast and slow motional regimes. The parameters obtained from computer simulations, i.e., the orientational distributions and conformations of the lipids, the motional correlation times, and the viscoelastic properties of the membranes, consistently describe the data for all specifically labeled lipids. A comparison of molecular order and dynamics in cholesterol-free and cholesterol-containing membranes allows direct monitoring of the effects of the steroid on the various physical properties of the bilayer.

Materials and Methods

Syntheses and Sample Preparation. Cholesterol and L-α-DMPC were obtained from Janssen Chimica and Sigma Chemie GmbH, respectively. Cholest-5-en-3-one was prepared from cholesterol by bromination, oxidation with sodium dichromate, and debromination with zinc as described (Fieser, 1963). Cholestenone was subsequently reduced with $LiAlD_4$ to yield cholesterol-*3*α-d_1 (Rosenfeld et al., 1954), which was separated from minor amounts of cholesterol-*3*β-d_1 by column chromatography and further purified by recrystallization from acetone. DMPC's specifically deuterated at positions 6, 13, and 14 of the *sn*-2 chain (*2*-[*6,6*-d_2]DMPC, 2-[*13,13*-d_2]-DMPC, and 2-[*14,14,14*-d_3]DMPC) were synthesized by enzymatic hydrolysis of L-α-DMPC with snake venom of *Crotalus adamanteus* (Sigma Chemie GmbH), followed by reacylation of the resulting 1-myristoyl-*sn*-glycero-3-phosphocholine with the corresponding deuterated acid anhydrides (Meier et al., 1986). The synthesis of specifically deuterated myristic acids is essentially described elsewhere (Das Gupta et al., 1982).

Multilamellar lipid dispersions were prepared by dissolving the phospholipid and cholesterol (3:2 molar ratio) in $CHCl_3$/MeOH. After partial removal of the solvent by a stream of nitrogen gas, the residual solvent was evaporated under vacuum (<1 Torr) for 24 h, and the dry lipid mixture (between 100 and 500 mg) was finally dispersed in 50 wt % of deuterium-depleted water (Aldrich Chemie). Homogenization of the sample was achieved by repeated shaking, freezing, and thawing. Macroscopically oriented samples were prepared by spreading about 70 mg of the dispersed lipid between 25 thin glass plates which were stacked on top of each other to fit in a 10-mm NMR sample tube. After drying and rehydrating the sample at 318 K (Jarrell et al., 1987), almost all of the lipid was uniformly aligned, as monitored by polarizing microscopy and NMR (^{31}P, ^{2}H). Essentially no degradation products could be detected in the samples by thin layer chromatography after the NMR measurements.

NMR Measurements. ^{2}H NMR experiments were performed on Bruker CXP 300 and MSL 300 spectrometers at 46.1 MHz (B_0 = 7 T). Spin–lattice relaxation times T_{1Z} were determined with composite (CP) inversion–recovery sequences $[(\pi\text{-CP})\text{-}t_1\text{-}(\pi/2)_x\text{-}t_2\text{-}(\pi/2)_y]$ (Heaton et al., 1988); the delay between $\pi/2$ pulses in the quadrupolar echo detection was typically set to t_2 = 30 μs. Transverse spin relaxation measurements were carried out applying quadrupole echo $[(\pi/2)_x\text{-}t_1\text{-}(\pi/2)_y]$ and Carr–Purcell–Meiboom–Gill (CPMG) pulse sequences $[(\pi/2)_x\text{-}t_1\text{-}[(\pi/2)_y\text{-}2t_1\text{-}]_n]$ (Luz & Meiboom, 1963; Blicharski, 1986; Bloom & Sternin, 1987) and recorded under high-power proton decoupling (γB_2 = 33 kHz). The $\pi/2$ pulse width was generally about 4 μs (10-mm coil) and 2.5 μs (5-mm coil). For macroscopically oriented samples, a home-built probe equipped with a goniometer was used. All experiments were recorded with quadrature detection and appropriate phase cycling schemes. Depending on the particular experiment between 400 and 40 000 scans were accumulated, the temperature of the sample being regulated to within ±0.5 K by a temperature control unit.

NMR Relaxation Model. The various ^{2}H NMR relaxation experiments were analyzed by using a comprehensive NMR model described in detail elsewhere (Müller et al., 1985; Meier et al., 1986; Stohrer et al., 1991). The model is based on the stochastic Liouville equation and considers internal, overall, and collective lipid motions (see Figure 1). The intramolecular motion consists of trans–gauche isomerization of individual segments in the phospholipid alkyl chain, which is represented by a jump process between discrete conformations. The intermolecular motion corresponds to restricted rotational diffusion of the molecules as a whole. Consequently, the dynamics of a single molecule can be characterized by the correlation times for reorientation of the diffusion tensor axis $\tau_{R\perp}$, rotation about this axis $\tau_{R\parallel}$, and intramolecular trans–gauche isomerization τ_J (see Figure 1).

Likewise, molecular order is described in terms of internal and external coordinates. The internal part accounts for different conformations and the external part for different orientations. Generally, there are only four conformational states accessible at a particular aliphatic chain segment (Flory, 1969). The corresponding populations n_1, ..., n_4 may be used to set up a segmental order matrix, which on diagonalization yields the segmental order parameters $S_{Z'Z'}$ and $S_{X'X'} - S_{Y'Y'}$. They express the ordering of the most ordered segmental axis and the anisotropy of that order, respectively (Meier et al., 1986). Within the limits of a completely disordered segment, all conformations are equally populated, resulting in an order parameter of $S_{Z'Z'} = 0$. At the other extreme, a fully extended chain is fixed to its all-trans conformation, and the order parameter becomes $S_{Z'Z'} = 1$.

The external part allows for different orientations of the lipid molecules with respect to the local director. In case of axially symmetric ordering, the normalized distribution function

$$f(\beta) = N_1 \exp(A \cos^2 \beta) \quad (1)$$

is employed, where β denotes the angle between the molecular long-axis Z and the director (Cotter, 1977). Note that the familiar order parameter S_{ZZ} is related to the coefficient A by a mean value integral

$$S_{ZZ} = \frac{1}{2} N_1 \int_0^{\pi} (3 \cos^2 \beta - 1) \exp(A \cos^2 \beta) \sin \beta \, d\beta \quad (2)$$

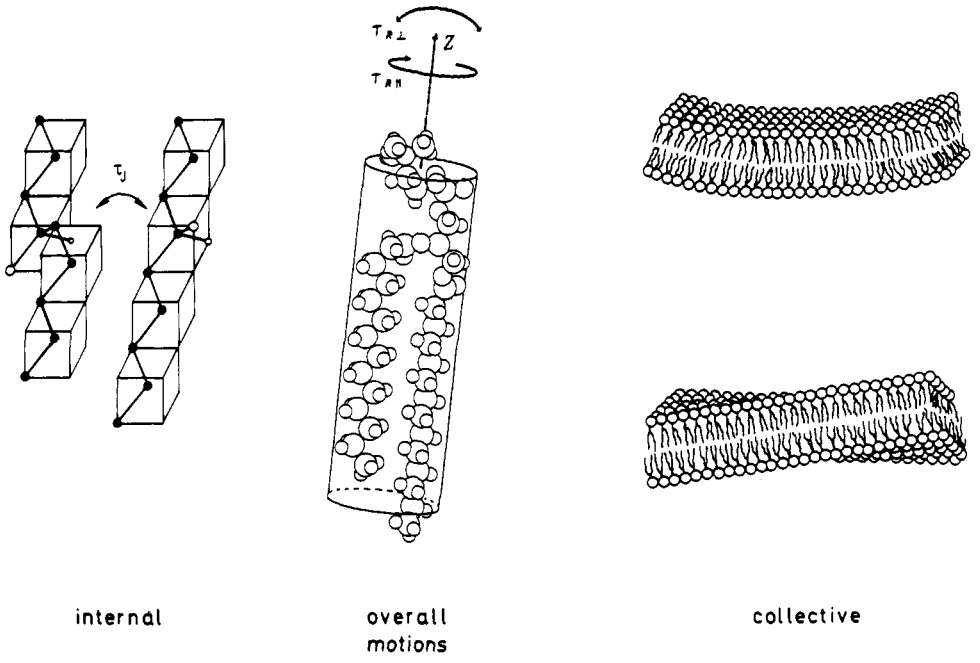

FIGURE 1: Schematic representation of the various motional modes in bilayer membranes: internal (τ_J), overall ($\tau_{R\parallel}$, $\tau_{R\perp}$), and collective lipid motions.

In addition to isolated motions of single molecules, collective motions of a large number of lipids (see Figure 1) were found to occur in liquid-crystalline bilayers (Rommel et al., 1988; Stohrer et al., 1991). They can be modeled as fluctuations of the instantaneous director with respect to its time-averaged orientation. Within the hydrodynamic theory, these time-dependent deformations of the ordered structure are analyzed in terms of a broad distribution of thermally activated modes (De Gennes, 1974). Using a small-angle approximation, the mean square fluctuations $\langle\theta^2(q)\rangle$ and relaxation times $\tau(q)$ of the elastic modes can be written as (Marqusee et al., 1984)

$$\langle\theta^2(q)\rangle = k_B T/(d\lambda_1^2 K q^2) \quad (3)$$

$$\tau(q) = \eta/(Kq^2) \quad (4)$$

Here k_B, d, λ_1, K, q, and η denote the Boltzmann constant, a coherence length associated with the bilayer thickness, the long wavelength cutoff of the elastic modes, the average elastic constant of the membrane, the wave vector of mode q, and the effective viscosity, respectively. Apparently, analysis of the collective lipid motions can provide information on the viscoelastic properties of the bilayer membranes.

Data Analysis. A Fortran program package was employed in the analysis of the ^{2}H NMR experiments. The numerical solution of the stochastic Liouville equation was achieved using the LANCZOS algorithm (Moro & Freed, 1981). Within the Redfield limit (Redfield, 1965), analytical expressions were applied in the analysis. The constant parameters in the calculations, obtained from fast rotational and rigid limit spectra, are summarized in Table I. They include a quadrupole coupling constant of e^2qQ/h = 169 kHz for the aliphatic deuterons and the Euler angles relating the magnetic and order (diffusion) tensor system in the four allowed conformational states at a particular chain segment (Meier et al., 1983, 1986). The orientation of the C–D bond vector in the rigid core of cholesterol-3α-d_1 is fully defined by one angle which was previously determined to be ϑ_K = 79° (Taylor et al., 1981).

The remaining adjustable parameters are the molecular correlation times $\tau_{R\perp}$, $\tau_{R\parallel}$, and τ_J, the viscoelastic parameters K and η of the membrane, the coefficient A reflecting the strength of the orienting potential, and the populations n_1, ..., n_4 of the conformational states. However, the latter need not all be evaluated. In general, the gauche conformations of a particular aliphatic chain segment are equally populated, corresponding to $n_2 = n_3$. From the normalization condition, we obtain $n_2 = (1 - n_1 - n_4)/2$. Consequently, there are only two unknown populations, namely, n_1 and n_4.

Table I: Constant Parameters Used in the Analysis of Pulsed Dynamic NMR Experiments of Deuterated Lipids in Bilayer Membranes

deuteron spin label	quadrup coupl const e^2qQ/h (kHz)	magnetic tensor orientation[a] conf state[b]	ϑ_K	ψ_K
2-[*6,6-d_2*]DMPC	169	1	90°	144.75°
2-[*13,13-d_2*]DMPC		2	90°	35.25°
		3	−144.75°	90°
		4	−35.25°	90°
2-[*14,14,14-d_3*]DMPC	56.3[c]	1	−144.75°	90°
		2	90°	144.75°
		3	90°	35.25°
		4	−35.25°	90°
cholesterol-3α-d_1	169		79°	arbitrary

[a] Euler angles relating magnetic and order (diffusion) tensor system (see Figures 1 and 2). [b] The numbers denote the four conformational states accessible at a particular aliphatic chain segment (Flory, 1969). [c] Motionally averaged owing to methyl group rotation.

In the fast motion regime ($T > T_M$), the parameters of orientational order A (S_{ZZ}) and segmental order n_1, n_4 ($S_{Z'Z'}$) are conveniently obtained from the quadrupolar splitting $\Delta\nu$ in the ^{2}H NMR spectrum. For deuterons attached to the *rigid* steroid ring system, $\Delta\nu$ is given by

$$\Delta\nu = (3/8)(e^2qQ/h)S_{ZZ}(3\cos^2\vartheta_K - 1)(3\cos^2\xi - 1) \quad (5)$$

where ξ is the angle between the time-averaged director and the magnetic field. For deuterons at a *flexible* chain segment, an analogous expression can be derived:

$$\Delta\nu = (3/8)(e^2qQ/h)S_{ZZ}(n_4 - n_1)(3\cos^2\xi - 1) \quad (6)$$

eliminating $(n_4 - n_1)$ as a free parameter if S_{ZZ} is known. Fortunately, S_{ZZ} can be evaluated separately from the angular variation of the spin–lattice relaxation time T_{1Z} (Mayer et al., 1990). Thus, the reduced line separation $\Delta\nu/S_{ZZ}$ indicates the conformational order at the particular labeled segment. Note, however, that this reduced splitting only contains in-

formation on $n_4 - n_1$, insufficient for the evaluation of the complete order matrix (Meier et al., 1986). Fortunately, there are two different ^{2}H spin labels, 2-[*13,13-d*$_2$]DMPC and 2-[*14,14,14-d*$_3$]DMPC, for the C-13 segment. They were both employed in determining conformational order at this position. The results for the C-6 segment are based on $n_4 = 0$, verified by independent NMR experiments (Meier et al., 1986).

The reliable evaluation of the dynamic parameters $\tau_{R\perp}$, $\tau_{R\parallel}$, τ_J, K, and η requires the detailed analysis of several independent relaxation experiments. In a bilayer membrane, a superposition of motional modes with different frequencies is observed. Employing different pulse sequences, each of which defines a specific dynamic window, often allows extraction of one motion dominating the particular relaxation. Fast reorientations of individual molecules account for spin–lattice relaxation in the conventional megahertz regime, since T_{1Z} is mostly affected by motions with correlation times equal to the inverse Larmor frequency, i.e., with $\tau_R \sim 10^{-9}$ s at 46.1 MHz (Rommel et al., 1988; Mayer et al., 1990). In contrast, much slower collective motions constitute the dominant transverse relaxation process above T_M, determining T_{2E} and T_{2E}^{CP} in this temperature region (Stohrer et al., 1991).

Since the motional processes are thermally activated, the variation of the sample temperature can be used to separate the various types of motions. Internal chain motions are too fast to have any significant effect on T_{1Z} at elevated temperatures but dominate the spin–lattice relaxation in the low-temperature regime where intermolecular motions are slow on the NMR time scale (Meier et al., 1986; Mayer et al., 1988). The position and absolute value of a minimum in the relaxation curve is highly indicative of the type of motion (Meier et al., 1986; Mayer et al., 1988). The dominant motion in one such region having been assigned, its temperature dependence is extrapolated into other regions where the situation may be more complex.

A further method for characterization of motions is based on the anisotropy of the relaxation times. For macroscopically aligned bilayers, T_{1Z}, T_{2E}, and T_{2E}^{CP} vary as a function of the sample orientation. It turns out that this variation is very dependent upon the character of the motion responsible for spin relaxation (Mayer et al., 1990; Stohrer et al., 1991).

Evaluation of the parameters K and η of the collective lipid motions is conveniently achieved by employing frequency-dependent transverse relaxation studies. As demonstrated elsewhere (Stohrer et al., 1991), the pulse frequency ($\omega = 1/t_1$) dispersion of $T_{2E}^{CP}(\omega)$ is not uniform over the entire frequency range. Two different regimes can be distinguished. For a broad interval, extending from the high- to the low-frequency cutoff ($\omega_1 < \omega < \omega_c$) of the elastic modes, a linear dispersion law is predicted (Stohrer et al., 1991):

$$1/T_{2E}^{CP}(\omega) \sim S_{CD}^2 \cos^2 \xi \sin^2 \xi [k_B T/(Kd)]\omega^{-1} \quad (7)$$

where $S_{CD} = (1/2)S_{ZZ}(n_4 - n_1)$ denotes the C–D bond order parameter. At lower frequencies ($\omega < \omega_1$), the relaxation dispersion should gradually disappear, and in the limit $\omega \rightarrow 0$ we expect $T_{2E}^{CP}(0)$ to be equal to T_{2E}, according to (Stohrer et al., 1991)

$$1/T_{2E}^{CP}(0) = 1/T_{2E} = (81/64)(e^2qQ/\hbar)^2 S_{CD}^2 \cos^2 \xi \sin^2 \xi [k_B T\eta/(\pi K^2 d q_1^2)] \quad (8)$$

The analysis is completed if the final parameter set consistently describes all relaxation experiments of the spin-labeled lipids, intermolecular and collective dynamics necessarily being independent of the label position within the molecule.

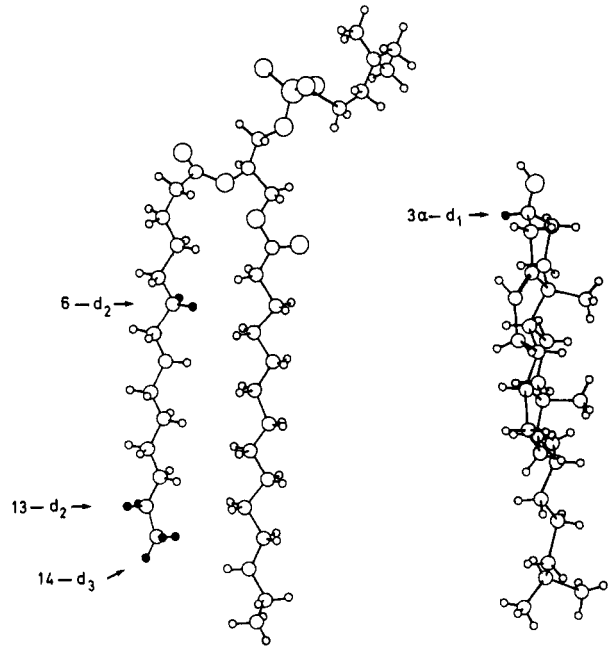

FIGURE 2: Molecular structures of DMPC and cholesterol with deuterium-labeled positions indicated by arrows.

RESULTS

Macroscopically oriented and unoriented bilayers of DMPC and cholesterol in a 3:2 molar ratio were studied by pulsed dynamic NMR techniques over a wide temperature range. The use of DMPC specifically deuterated at the 6-, 13-, or 14-position of the *sn*-2 chain and cholesterol labeled at the 3α-position of the rigid steroid ring system (see Figure 2) allows for a proper dynamic characterization of both lipid components within the bilayer membrane. For comparison, corresponding data of pure DMPC bilayers obtained in a previous investigation under the same experimental conditions (Mayer et al., 1988) have been included. Thus, this study not only extensively covers various aspects of the dynamic organization in phospholipid/cholesterol membranes but also directly focuses on the changes brought about by the addition of cholesterol into the lipid bilayer.

Type and Time Scale of Motions. Typical quadrupole echo lineshapes of multilamellar 2-[*6,6-d*$_2$]DMPC in the absence (left row) and presence of 40 mol % cholesterol (right row) are shown in Figure 3a. The three different temperatures characterize the L_α, P_β', and L_β' phase of pure DMPC bilayers. The spectra at 303 K exhibit a narrow axially symmetric powder pattern for DMPC in either membrane. The strongly increased quadrupolar splitting for 2-[*6,6-d*$_2$]DMPC in cholesterol-containing bilayers corresponds to the overall ordering effect of the steroid in this phase. Cooling below the main transition T_M at 297 K causes drastic changes in the pure DMPC spectrum. It now discloses a broad featureless line shape indicative of slow molecular dynamics, which gradually changes to a rigid limit powder spectrum (not shown). As was found previously, addition of 40 mol % cholesterol eliminates the main transition of the phospholipid, and a fast motional symmetric powder pattern persists down to temperatures well below T_M in the presence of cholesterol. Upon further cooling, a broad gel phase spectrum finally appears at 263 K, overlapping the narrow component.

Figure 3b shows temperature-dependent quadrupole echo spectra for 2-[*6,6-d*$_2$]DMPC and cholesterol-*3α-d*$_1$ in a mixed multilamellar dispersion. Both lipid components exhibit symmetric fast motional spectra above 273 K. Decreasing the temperature results in the gradual transition of the narrow

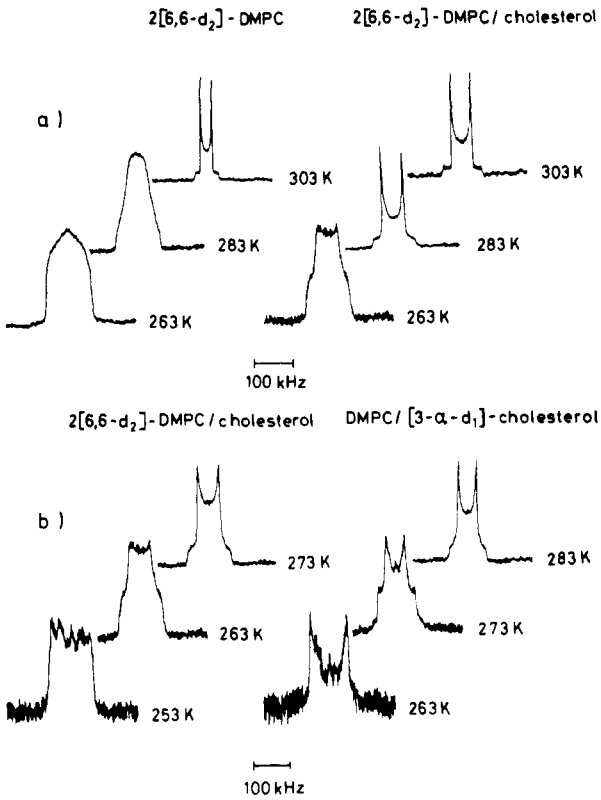

FIGURE 3: (a) Experimental ^2H NMR spectra of 2-[*6,6-d*$_2$]DMPC in pure DMPC bilayers (left row) and in DMPC/cholesterol mixed membranes (40 mol % cholesterol, right row) at three different temperatures. (b) Experimental ^2H NMR spectra of 2-[*6,6-d*$_2$]DMPC (left row) and cholesterol-*3α-d*$_1$ (right row) in DMPC/cholesterol mixed membranes (40 mol % cholesterol) at three different temperatures. (a and b) All spectra refer to multilamellar lipid dispersions.

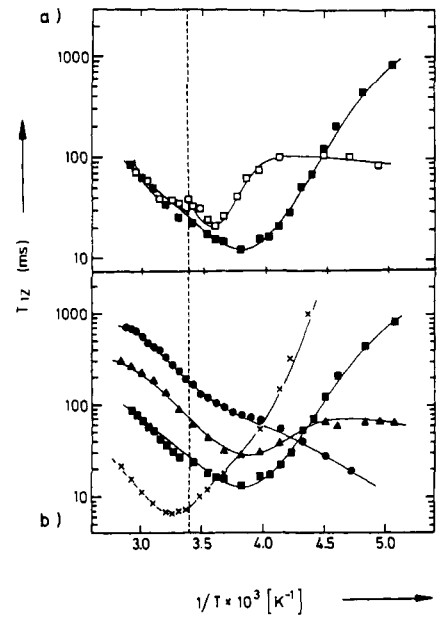

FIGURE 4: (a) Temperature dependence of the longitudinal ^2H spin relaxation times T_{1Z} of 2-[*6,6-d*$_2$]DMPC in bilayer membranes with (■) and without (□) 40 mol % cholesterol. (b) Temperature dependence of the longitudinal ^2H spin relaxation times T_{1Z} of 2-[*6,6-d*$_2$]DMPC (■), 2-[*13,13-d*$_2$]DMPC (▲), 2-[*14,14,14-d*$_3$]DMPC (●), cholesterol-*3α-d*$_1$ (×) in DMPC/cholesterol mixed membranes (40 mol % cholesterol). (a and b) All relaxation times refer to multilamellar lipid dispersions. The dashed line indicates the main transition of pure DMPC bilayers. The solid lines represent best fit simulations of the relaxation times, performed as described in the text (see Materials and Methods).

"fluid" component into a broad gel-like component, and two overlapping powder patterns are observed within a temperature range of about 20 K. At 273 K the broad component in the cholesterol-*3α-d*$_1$ spectrum exhibits a quadrupolar splitting of about 100 kHz, indicating that axial rotation has ceased on the NMR time scale for this lipid population. However, some motional averaging still occurs, reducing the maximum splitting of 125 kHz expected for a static Pake diagram. Interestingly, the broad component in the 2-[*6,6-d*$_2$]DMPC spectrum is first found only at 263 K, i.e., 10 K below the appearance of the immobilized cholesterol species. Apparently, cholesterol molecules first freeze out preferentially, followed by phospholipid upon further cooling.

The overlapping components in the DMPC/cholesterol bilayers are easily differentiated by their respective relaxation behavior. Quadrupole echo spectra, taken at different pulse separation times t_1 (not shown), clearly indicate that in both cases the "fluid" component relaxes much faster, only the broad component being observable at $t_1 \geq 70$ μs.

The spin–lattice relaxation times T_{1Z}, shown in Figure 4, were obtained by recording the echo amplitude of an inversion–recovery sequence as a function of the delay time between the π and first $\pi/2$ pulse (see NMR Measurements). They refer to DMPC deuterated at positions 6, 13, and 14 of the *sn*-2 chain and to cholesterol-*3α-d*$_1$ in unoriented multilamellar dispersion. Generally, T_{1Z} is defined as the time it takes for the echo amplitude to decay to $1/e$ of its original value. This definition includes nonexponential decay, as expected for the unoriented samples.

Comparison of the relaxation curves for 2-[*6,6-d*$_2$]DMPC in bilayers with (filled symbols) and without (open symbols) 40 mol % cholesterol clearly indicates changes in the relaxation behavior (see Figure 4a). As expected, no discontinuity is observed at T_M (dashed line) for the mixed lipid system. Instead, T_{1Z} of 2-[*6,6-d*$_2$]DMPC/cholesterol continuously decreases with decreasing temperature until a broad and deep minimum is reached at 263 K. This pronounced minimum is also observed for the pure lipid system at slightly elevated temperature (273 K). The measured T_{1Z} values at the minimum are not compatible with reorientation of the lipid molecules as a whole. Rather, they indicate two-site rotational jumps of the *sn*-2 chain in the plane of the membrane, associated with the *isomerization at the C-2 segment* (Mayer et al., 1988). On further cooling, the T_{1Z} values for 2-[*6,6-d*$_2$]DMPC/cholesterol continuously increase, while those for the pure system level off to a plateau, resulting from *trans–gauche isomerization at C-6* (Mayer et al., 1988).

Figure 4b depicts T_{1Z} relaxation curves for various spin-labeled lipids in cholesterol-containing dispersions. We see that the temperature dependences of 2-[*6,6-d*$_2$]DMPC, 2-[*13,13-d*$_2$]DMPC and 2-[*14,14,14-d*$_3$]DMPC are quite similar above the common T_{1Z} minimum of the former two. The further course, however, strongly depends on the labeled segment. While T_{1Z} values for 2-[*6,6-d*$_2$]DMPC continuously increase upon cooling, those of 2-[*13,13-d*$_2$]DMPC level off to a plateau. In contrast, T_{1Z} of 2-[*14,14,14-d*$_3$]DMPC further decreases by lowering the temperature due to *methyl group rotation* (Meier et al., 1986). Interestingly, the relaxation curves for DMPC deuterated at the 13- and 14-position flatten toward their *high-temperature end.* This behavior can be rationalized by overall lipid motions becoming increasingly effective in T_{1Z} relaxation above T_M.

The T_{1Z} relaxation data of cholesterol-*3α-d*$_1$ show a very deep minimum at 308 K and a subsequent steep increase of the T_{1Z} values toward lower temperatures. Similar T_{1Z} minima were found for various deuterated cholesterols in DMPC (Dufourc & Smith, 1986) and egg lecithin membranes (Taylor

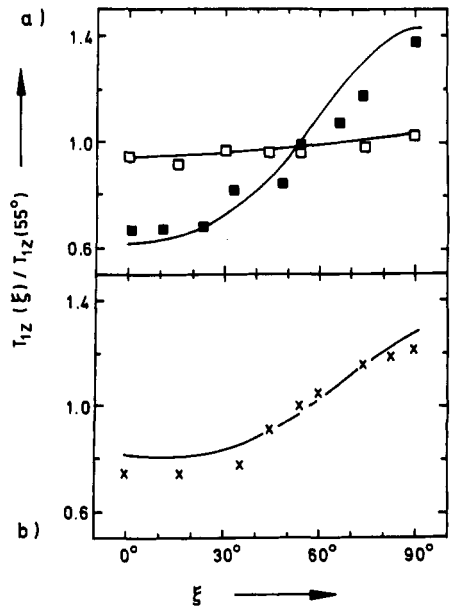

FIGURE 5: (a) Angular dependence of the longitudinal ^{2}H spin relaxation times T_{1Z} of 2-[*6,6-d*$_2$]DMPC in macroscopically oriented DMPC membranes with (■) and without (□) 40 mol % cholesterol. Temperature T = 308 K. (b) Angular dependence of the longitudinal ^{2}H spin relaxation times T_{1Z} of cholesterol-*3α-d*$_1$ (×) in macroscopically oriented DMPC/cholesterol mixed membranes (40 mol % cholesterol). Temperature T = 328 K. (a and b) The solid lines represent best fit simulations of the relaxation times, performed as described in the text (see Materials and Methods). ξ is the angle between bilayer normal (time-averaged director) and magnetic field.

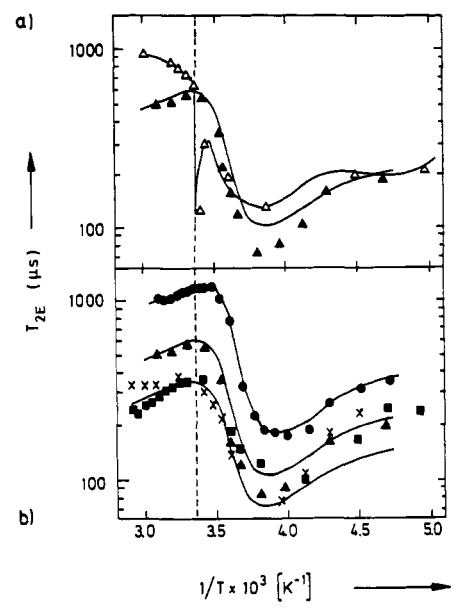

FIGURE 6: (a) Temperature dependence of the transverse ^{2}H spin relaxation times T_{2E} of 2-[*13,13-d*$_2$]DMPC in bilayer membranes with (▲) and without (△) 40 mol % cholesterol. (b) Temperature dependence of the transverse ^{2}H spin relaxation times T_{2E} of 2-[*6,6-d*$_2$]DMPC (■), 2-[*13,13-d*$_2$]DMPC (▲), 2-[*14,14,14-d*$_3$]DMPC (●), and cholesterol-*3α-d*$_1$ (×) in DMPC/cholesterol mixed membranes (40 mol % cholesterol). (a and b) All relaxation times refer to multilamellar lipid dispersions. The dashed line indicates the main transition of pure DMPC bilayers. The solid lines represent best fit simulations of the relaxation times, performed as described in the text (see Materials and Methods).

et al., 1982). The observed T_{1Z} values at the minimum are compatible with rotations of the steroid molecules as a whole.

The anisotropy of the spin–lattice relaxation time T_{1Z} sensitively reflects the type of motion responsible for longitudinal spin relaxation at a particular temperature. Figure 5a depicts the angular dependence of T_{1Z} for 2-[*6,6-d*$_2$]DMPC in the two bilayer systems. The data refer to T = 308 K and are plotted as a function of the orientation of the glass plate normal with respect to the magnetic field. Since no collective lipid tilt exists in the L_α phase, the glass plate normal coincides with the time-averaged director. In the absence of cholesterol, the dependence of T_{1Z} on the director orientation is marginal. Only a slight increase of T_{1Z} toward the ξ = 90° orientation can be detected. In contrast, the 2-[*6,6-d*$_2$]DMPC/cholesterol sample exhibits a pronounced angular dependence, i.e., $T_{1Z}(90°)/T_{1Z}(0°)$ = 2.2 (Mayer et al., 1990). Similar results have been obtained from partially relaxed (T_{1Z}) ^{2}H NMR spectra of unoriented phospholipid/cholesterol membranes (Siminovitch et al., 1985, 1988).

Analysis of the angular variation clearly shows that *restricted rotational diffusion* of individual lipid molecules constitutes the dominant longitudinal relaxation process above T_M (Mayer et al., 1990). Furthermore, it turns out that the orientational order of the lipid molecules is the crucial factor determining the T_{1Z} anisotropy. Apparently, there is a considerable increase of this order upon addition of 40 mol % cholesterol (Mayer et al., 1990).

Figure 5b depicts the angular dependence of T_{1Z} for cholesterol-*3α-d*$_1$ in macroscopically oriented mixed bilayers. The data refer to T = 328 K and nine different orientations of director with respect to the magnetic field. One recognizes that the spin–lattice relaxation of the deuterated cholesterol exhibits a pronounced angle dependence, i.e., $T_{1Z}(90°)/T_{1Z}(0°)$ = 1.5, in good agreement with previous observations (Bonmatin et al., 1988). Again, this finding indicates that *overall reorientations* of individual lipid molecules represent the dominant relaxation process (Mayer et al., 1990).

Spin–spin relaxation times T_{2E} determined by quadrupolar echo sequences are plotted in Figure 6 as a function of $1/T$ for the various deuterated lipids. As before, these relaxation times are defined as the time it takes for the echo amplitude to decay to $1/e$ of its original value. This definition allows for nonexponential decay, as observed for the powder samples particularly at higher temperatures ($T > T_M$). As shown for 2-[*13,13-d*$_2$]DMPC (Figure 6a), the characteristic relaxation curve for the pure phospholipid (open symbols), exhibiting an abrupt decrease of T_{2E} at the main transition and a subsequent local maximum just below the pretransition (Meier et al., 1986; Mayer et al., 1988), is significantly altered upon addition of cholesterol. One sees that the T_{2E} values in cholesterol-containing bilayers (filled symbols) first increase with decreasing temperature, reaching a maximum at 293 K, then continuously decrease and finally pass through a deep minimum at 253 K.

Similar transverse relaxation curves are found for all spin-labeled phospholipids and cholesterol-*3α-d*$_1$ in the mixed bilayers, implying common motional modes (Figure 6b). Note the exceptional temperature dependence above 293 K, where all T_{2E} values increase with decreasing temperature, and the pronounced T_{2E} minimum at 253 K. A value of $(T_{2E})_{min} \sim 75$ μs is one of the shortest transverse relaxation times observed for ^{2}H nuclei in C–^{2}H bonds. Higher values for 2-[*14,14,14-d*$_3$]DMPC, also found in pure DMPC membranes, reflect fast methyl group rotation, which effectively averages the quadrupole coupling constant to one-third of its original value (Meier et al., 1983, 1986; Mayer et al., 1988).

The T_{2E} anisotropy of 2-[*6,6-d*$_2$]DMPC in cholesterol-containing bilayers is shown in Figure 7. The data refer to T = 333 K (Figure 7a) and T = 273 K (Figure 7b) and characterize five different orientations of director and magnetic field. Clearly, the angle dependence significantly differs for the two temperatures, indicating that different types of motions

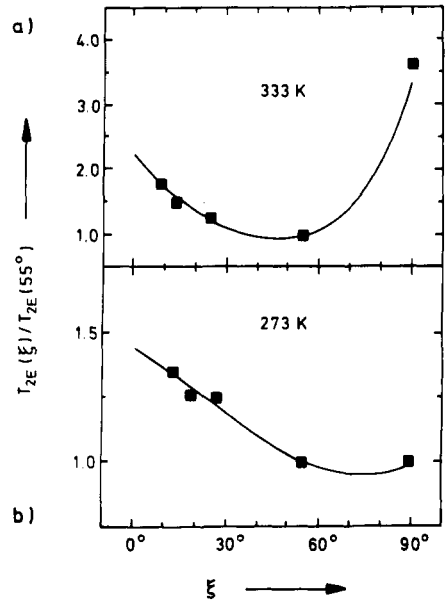

FIGURE 7: Angular dependence of the transverse ^2H spin relaxation times T_{2E} of 2-[6,6-d_2]DMPC (■) in macroscopically oriented DMPC/cholesterol mixed membranes (40 mol % cholesterol) at (a) T = 333 K and (b) T = 273 K. The solid lines represent best fit simulations of the relaxation times, performed as described in the text (see Materials and Methods). ξ is the angle between the bilayer normal (time-averaged director) and the magnetic field.

constitute the dominant transverse relaxation process. While the T_{2E} anisotropy in the low-temperature region is fully consistent with *rotational diffusion* of individual molecules, the characteristic T_{2E} minimum at $\xi \sim 45°$ indicates *collective motional modes*, dominating spin–spin relaxation at higher temperatures.

Figure 8 depicts the pulse frequency ($\omega = 1/t_1$) dependence of the transverse relaxation time T_{2E}^{CP} obtained from CPMG pulse sequences (Bloom & Sternin, 1987; Stohrer et al., 1991). The data refer to 2-[6,6-d_2]DMPC in pure (open symbols) and cholesterol-containing bilayers (filled symbols) at T = 318 K and ξ = 55°. They have been obtained from powder samples employing a deconvolution procedure (Dufourc et al., 1992). Apparently, in both cases there is a broad interval where $T_{2E}^{CP}(\omega)$ is proportional to ω^1. Such a linear frequency dependence is not compatible with a single motional process, characterized by a quadratic dispersion law. Rather, the observed frequency dependence indicates a superposition of relaxation contributions from a large number of different modes (Stohrer et al., 1991). Prime candidates for such motions are *collective order fluctuations* (see Figure 1). Note that cholesterol has a significant effect on these cooperative motions, increasing T_{2E}^{CP} by nearly a factor of 2.

Molecular and Viscoelastic Properties. In summary, three different motional classes can be distinguished in the ^2H NMR experiments, *i.e., internal, overall, and collective lipid motions* (see Figure 1). The internal motions consist of *trans–gauche isomerization* of individual segments in the phospholipid alkyl chain. They are the fastest processes in the hierarchy of time. The overall lipid motions, occurring on a considerably longer time scale, can be interpreted as *restricted rotational diffusion* of the molecules as a whole. The slowest motion affecting the ^2H NMR observables is assigned to *collective order fluctuations* and is only detected at higher temperatures above T_M in the bilayer membranes.

Once the nature and rank in the hierarchy of time is determined for each motion, the next step is to perform the proper averaging of the quadrupole tensor starting with the

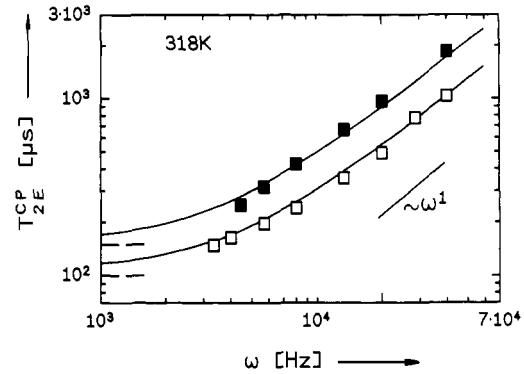

FIGURE 8: Pulse frequency ($\omega = 1/t_1$) dependence of the transverse ^2H spin relaxation times T_{2E}^{CP} obtained for DMPC/cholesterol mixed membranes (■, 40 mol % cholesterol) and pure DMPC bilayers (□) in Carr–Purcell–Meiboom–Gill pulse trains. The relaxation times refer to 2-[6,6-d_2]DMPC, T = 318 K, and ξ = 55°. Dashed lines indicate the limiting values for $\omega \rightarrow 0$, i.e., $T_{2E}^{CP}(0) \equiv T_{2E}$. The solid lines represent best fit simulations of the relaxation times, performed as described in the text (see Materials and Methods). ξ is the angle between bilayer normal (time-averaged director) and magnetic field.

fastest process (Dufourc et al., 1992). The NMR observables such as T_{1Z}, T_{2E}, T_{2E}^{CP}, and line shapes are then calculated by employing the NMR model outlined above. An iterative fit of several pulse and orientation-dependent experiments for any given temperature provides reliable values for the adjustable parameters, i.e., the order parameters of the lipid molecules (see Figure 9), the correlation times and activation energies of individual lipid motions (see Figures 10–12 and Table II), and the viscoelastic parameters characterizing collective lipid motions (see Table III). Best fit simulations, represented by solid lines in Figures 4–8, agree favorably with their experimental counterparts. Note that the relaxation behavior of the different spin labels is reproduced with the same set of parameters, which are discussed in more detail in the following.

Discussion

Molecular Order. The molecular order in lipid bilayers, comprising inter- and intramolecular contributions, is conveniently described by the orientational order parameter S_{ZZ} and the segmental order parameter $S_{Z'Z'}$ (see NMR Relaxation Model). Values for these order parameters in pure (open symbols) and mixed bilayers (filled symbols), obtained by the above analysis, are shown in Figure 9 for a wide temperature range. Dashed lines indicate the main transition of pure DMPC dispersions. Generally, the maximum error for both order parameters is ±5%.

In Figure 9a the orientational order parameters S_{ZZ} are plotted as a function of temperature. Apparently, above T_M orientational ordering of the phospholipids is significantly increased upon addition of cholesterol, S_{ZZ} being raised from 0.68 in pure DMPC membranes to 0.85 in mixed bilayers at 308 K. By lowering the temperature, S_{ZZ} *continuously* increases in the cholesterol-containing bilayers without any indication of microscopic heterogeneity. This result is consistent with the recently established phase diagram of phospholipid/cholesterol mixtures (Vist & Davis, 1990; Ipsen et al., 1987), which predicts a broad liquid ordered or β-phase at high cholesterol concentrations. In contrast, for pure DMPC dispersions two components are observed below T_M with different orientational order (Meier et al., 1986; Mayer et al., 1988; Dufourc et al., 1992). Note that in the low-temperature region S_{ZZ} values in mixed membranes are considerably smaller than those found for pure DMPC bilayers, thus allowing for noticeable fluctuations of the lipid molecules. Interestingly, cholesterol exhibits orientational order parameters (crosses)

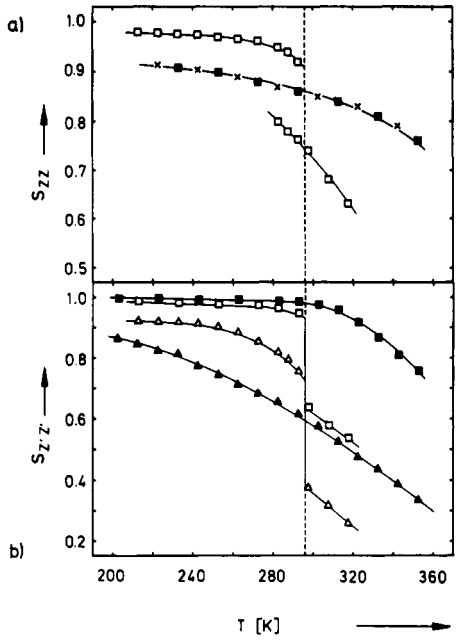

FIGURE 9: (a) Temperature dependence of the orientational order parameters S_{ZZ} for DMPC (■) and cholesterol (×) in DMPC/cholesterol mixed membranes (40 mol % cholesterol) and for DMPC (□) in pure phospholipid bilayers. (b) Temperature dependence of the segmental order parameters $S_{Z'Z'}$ at the 6- (■) and 13-position (▲) of the phospholipid *sn*-2 chain in DMPC/cholesterol mixed membranes (40 mol % cholesterol). The corresponding values for $S_{Z'Z'}$ in pure DMPC bilayers are represented by open symbols (□, △). (a and b) The dashed line indicates the main transition of pure DMPC membranes.

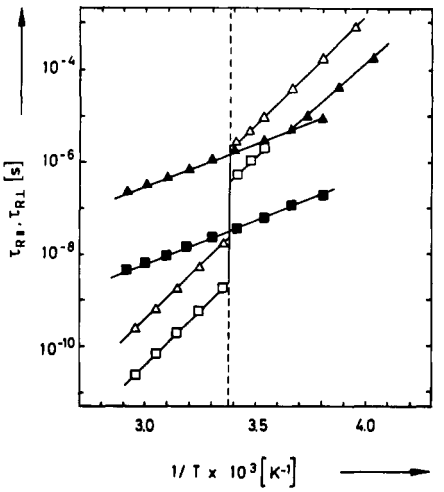

FIGURE 10: Arrhenius plot of the correlation times $\tau_{R^\parallel}$ (■) and $\tau_{R^\perp}$ (▲), characterizing overall rotation and fluctuation of DMPC in DMPC/cholesterol mixed membranes (filled symbols, 40 mol % cholesterol) and in pure DMPC bilayers (open symbols). The dashed line indicates the main transition of pure DMPC membranes.

equal to those found for the phospholipids in mixed membranes over the whole temperature range investigated.

Figure 9b depicts the temperature variation of $S_{Z'Z'}$, describing conformational order at the 6- (squares) and 13-position (triangles) of the *sn*-2 chain. For both cholesterol-free and cholesterol-containing bilayers, conformational order decreases toward the end of the chains, reflecting the well-known order gradient (Seelig & Seelig, 1974; Davis 1979; Lafleur et al., 1990; Sankaram & Thompson, 1990). However, the number of gauche conformers along the chain is significantly reduced by cholesterol above T_M, and the order parameters $S_{Z'Z'}$ for the 6- and 13-position are raised from 0.58 to 0.97 and from 0.32 to 0.55, respectively (308 K). Lowering the temperature continuously increases conformational order at both positions in mixed bilayers without any discontinuities at T_M. Note, however, that the limiting value of $S_{Z'Z'} \sim 1.0$, corresponding to an all-trans chain, is already obtained at T_M for the 6-position. In contrast, order parameters for the 13-position are well below 1.0 even at very low temperatures, implying increased gauche populations below T_M in the presence of the steroid.

It is apparent that the overall ordering effect of cholesterol above T_M is due to substantially restricted amplitudes in the rigid body fluctuations as well as to increased trans probabilities along the phospholipid alkyl chain. Interestingly, at the high cholesterol concentration employed, steroid and phospholipid exhibit molecular fluctuations of *equal amplitudes* over a wide temperature range. In contrast, for DMPC membranes of lower cholesterol content, significant differences in the wobbling amplitudes have been reported (Dufourc et al., 1984). However, intramolecular disorder at the phospholipid alkyl segments was not taken into account in this study.

The conformational order at the 6-position of the DMPC *sn*-2 chain is strongly increased by the rigid steroid ring system, which faces the upper part of the alkyl chain (see Figure 2) and prevents segments in the plateau region from forming unfavorable gauche conformations. Thus, just above T_M, the methylene units near the carbonyl oxygen are in an almost perfectly ordered state. Toward the chain end gauche conformers become increasingly populated, resulting in a lower segmental order at the 13-position. Note, however, that for $T > T_M$ incorporation of cholesterol also substantially increases $S_{Z'Z'}$ near the chain end, which is in close contact to the aliphatic C_8 side group of the sterol (see Figure 2). Thus, similar to the steroid ring system, the C_8 residue exerts ordering effects on terminal alkyl segments, implying a relatively rigid cholesterol side chain within the lipid bilayer (Dufourc et al., 1984).

Apparently, increased trans populations along the phospholipid alkyl chain (Davies et al., 1990), which effectively reduce the cross-sectional area per chain and thus decrease the bilayer compressibility (Needham et al., 1988), give rise to the condensing effect of cholesterol. Likewise, the decreased number of chain defects, formed by successive gauche conformers (Butler et al., 1970; Träuble, 1971), might be responsible for the reduced nonspecific permeation of small molecules or ions in cholesterol-containing bilayers (Papahadjopoulos et al., 1971; De Kruyff et al., 1972).

At high concentrations cholesterol is found to completely eliminate the liquid-crystalline-to-gel phase transition, which is accompanied by a rearrangement of the alkyl chains into an ordered lattice (Vist & Davis, 1990). Correspondingly, no abrupt increase in molecular order is observed at T_M in the mixed lipid bilayers. Thus, orientational and conformational order parameters are generally well below those found for gel-state DMPC, and hence low-amplitude wobbling motions are expected to persist even at very low temperatures. Apparently, the sterol prevents the phospholipid from forming a crystalline state with highly ordered, fully extended, all-trans chains, the less dense molecular packing giving rise to increased intermolecular distances within the bilayer (Hui & He, 1983). Similarly, 20 mol % cholesterol is sufficient to suppress the formation of the highly ordered subphase, as found previously (Boyanov et al., 1986).

Phospholipid Motions. In Figure 10 the correlation times $\tau_{R^\parallel}$ and $\tau_{R^\perp}$, characterizing the overall phospholipid dynamics, are plotted as a function of $1/T$. They refer to pure DMPC membranes (open symbols) and DMPC/cholesterol mixed

bilayers (filled symbols). The dashed line indicates the main transition of multilamellar DMPC. Inspection of the logarithmic plots reveals a large dynamic range extending over eight orders of magnitude. The uncertainty in correlation times is generally <20%.

In all cases, linear Arrhenius plots are obtained within a particular phase. As expected from the relaxation data, no discontinuity is observed for the cholesterol-containing membrane at T_M, in agreement with the established phase diagram (Vist & Davis, 1990; Ipsen et al., 1987). Instead, both intermolecular motions gradually slow down upon cooling up to 30 K below T_M, with correlation times $\tau_{R\parallel}$ ranging from 10^{-8} to 10^{-7} s. The constant anisotropy ratio $\tau_{R\perp}/\tau_{R\parallel} = 50$ in the DMPC/cholesterol system is increased by a factor of 5 when compared to the pure membrane, implying a change in the anisotropic molecular interactions within the bilayer.

On the basis of reports of subtle changes in the lateral (Rubenstein et al., 1979; Thompson & Axelrod, 1980) and rotational diffusion (Kawato et al., 1978; Kar et al., 1985) of probe molecules in cholesterol-containing bilayers, it was concluded that the steroid has little influence on the membrane fluidity in the high-temperature region (Bloom & Mouritsen, 1988). The present study indicates that cholesterol preserves relatively fast phospholipid rotation well below T_M, as is evidenced by axially symmetric quadrupole echo spectra even at 273 K (see Figure 3b). Nevertheless, both intermolecular motions are slowed down in the mixed membranes, correlation times for long-axis rotation being increased from $\tau_{R\parallel} = 0.5$ ns to $\tau_{R\parallel} = 18$ ns at 308 K. However, despite this apparent decrease in the rotational diffusion rates, cholesterol-containing bilayers behave like two-dimensional liquids with relatively high fluidity (Bloom & Mouritsen, 1988) and zero surface shear restoring forces (Needham et al., 1988).

The angle dependence of the spin–spin relaxation time T_{2E} indicates that rotational diffusion is the dominant transverse relaxation process down to 273 K (see Figure 7b). Below this temperature, an additional phospholipid component appears, exhibiting only slow molecular fluctuations with correlation times of $\tau_{R\perp} > 10^{-6}$ s. The fraction of this "immobilized" phospholipid increases with decreasing temperature, and at about 253 K, depending on the incubation period and the thermal history of the sample, only the motionally restricted component is left. A similar coexistence of fluid- and gel-like phospholipids is also observed in the $P_{\beta'}$ phase of multilamellar DMPC (Mayer et al., 1988). Likewise, ^{13}C and ^{2}H NMR studies on dipalmitoylphosphatidylethanolamine/cholesterol mixed bilayers revealed two distinct phospholipid components at lower temperatures (Blume & Griffin, 1982). Hysteresis effects indicate that the condensation of the phospholipids, involving the rearrangement into a tighter molecular packing, represents a kinetically controlled noncooperative process.

Failure to detect this transformation in DSC measurements is likely due to the particular nature of this process. Note that the superimposed powder spectra of 2-[6,6-d_2]DMPC are considerably broadened at 263 K, indicating exchange between the two distinct phospholipid components (see Figure 3b). In contrast, cholesterol-3α-d_1 at 273 K exhibits two overlapping powder spectra without any sign of exchange broadening (see Figure 3b). While a detailed structural interpretation of these findings is rather speculative at present, differences in the exchange rates of the two membrane components may reflect the specific spatial organization of the lipids within this binary system (Presti et al., 1982).

Activation energies for the various motions, determined from the slopes of the straight lines in the Arrhenius plots, are listed in Table II. It can be seen that incorporation of 40 mol % steroid results in a considerable decrease of the activation energies in the high-temperature region from $E_R = 90$ kJ/mol to $E_R = 35$ kJ/mol. Lowering the activation energy for lipid rotational diffusion enables cholesterol to maintain the fluid-like state of the bilayer over a wide range of temperature, pressure, and ionic strength, thus acting as effective buffer against outer physical and chemical changes.

Table II: Activation Energies of Individual Lipid Motions in Bilayer Membranes

lipid	activation energies (kJ/mol)[a]			
	$E_{R\perp}$	$E_{R\parallel}$	E_J (C-6)	E_J (C-13)
pure DMPC	90 ± 5	90 ± 5	15 ± 3[b] 8 ± 1[c]	15 ± 3[b] 8 ± 1[c]
DMPC with 40 mol % cholesterol	35 ± 4[d] 80 ± 5[e]	35 ± 4[d]	10 ± 1	7 ± 1
cholesterol	38 ± 2[d] 80 ± 5[e]	38 ± 2[d]		

[a] $E_{R\perp}$ and $E_{R\parallel}$ refer to long-axis fluctuation and rotation, respectively. E_J (C-6) and E_J (C-13) denote the activation energies for trans–gauche isomerization at the C-6 and C-13 segment. [b] Liquid-crystalline phase (L_α). [c] Intermediate ($P_{\beta'}$) and gel phase ($L_{\beta'}$). [d] $T > 273$ K. [e] $T < 253$ K.

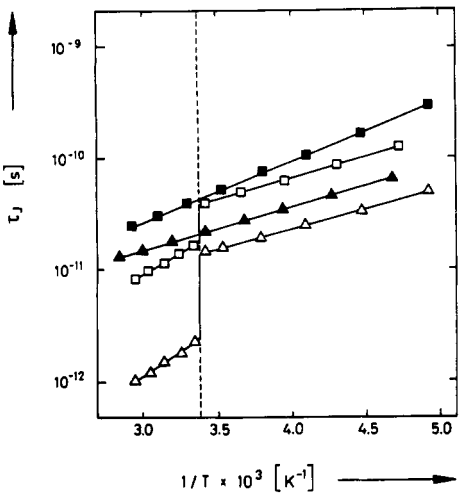

FIGURE 11: Arrhenius plot of the correlation times τ_J, characterizing trans–gauche isomerization of DMPC at the 6- (■) and 13-position (▲) of the *sn*-2 chain. Filled symbols refer to DMPC/cholesterol mixed membranes (40 mol % cholesterol), while open symbols denote pure DMPC bilayers. The dashed line indicates the main transition of pure DMPC membranes.

As expected for the more densely packed low-temperature state, small-amplitude librational motions exhibit increased activation energies of $E_R = 80$ kJ/mol, similar to those found for pure gel-phase phospholipid. However, correlation times for these molecular fluctuations are lowered by one order of magnitude in cholesterol-containing bilayers, again implying a less tight molecular packing in these mixed systems. The striking T_{2E} minimum in the relaxation curves of the phospholipids at 253 K (see Figure 6) can be attributed to small-angle librations, which are in the most sensitive dynamic range for T_{2E} relaxation at this temperature.

Arrhenius plots of the correlation times τ_J for the intramolecular motions are shown in Figure 11. They refer to trans–gauche isomerization at the 6- (squares) and 13-segment (triangles) of the phospholipid *sn*-2 chain in pure (open symbols) and cholesterol-containing bilayers (filled symbols). These motions are considerably faster than overall molecular reorientations, and even in the low-temperature region correlation times of $\tau_J \leq 10^{-10}$ s prevail. Despite the larger error

in determining such short correlation times, a pronounced *mobility gradient* along the hydrocarbon chains is evident, τ_J decreasing from the C-6 to the C-13 segment for either membrane.

For the mixed bilayers, linear Arrhenius plots are observed over the whole temperature range. While below T_M correlation times are only slightly affected, the τ_J values significantly increase above the phospholipid main transition in the presence of the sterol. Thus, trans–gauche isomerization rates at both positions are lowered by cholesterol to values typical of pure gel-phase lipid. Note that the steroid slows down isomerization at the terminal 13-segment by about one order of magnitude while the corresponding decrease in the isomerization rate at the 6-position is less pronounced. The significant restriction in flexibility for the terminal alkyl segment further corroborates findings of a relatively rigid cholesterol side chain, which effectively hampers reorientations at the phospholipid chain end.

Activation energies for trans–gauche isomerizations are also listed in Table II. As expected, the E_J values are substantially smaller than those found for overall molecular reorientation. Obviously, incorporation of cholesterol leads to a similar decrease in the activation energy as is observed for cholesterol-free bilayers on going from the liquid-crystalline to the gel phase. Addition of the steroid thus results in alkyl chain motions typical for the paracrystalline gel phase.

Cholesterol Motions. From an analysis of the spin–lattice relaxation anisotropy, it was concluded that cholesterol reorientation occurs via large angle jumps rather than via continuous diffusion (Bonmatin et al., 1988, 1990). However, for either mechanism a simplified model was employed, assuming perfect orientational ordering, i.e., $S_{ZZ} = 1$, and thus neglecting relaxation contributions from long-axis fluctuations (Siminovitch et al., 1985, 1988). On the other hand, a diffusive model considering these fluctuations (Mayer et al., 1990) favorably accounts for the T_{1Z} anisotropy (Brown, 1990; this work). As in the case of the phospholipid, we therefore assume that anisotropic rotational diffusion is the dominant motional process of cholesterol. Consequently, the molecular dynamics can be characterized by the two correlation times $\tau_{R\perp}$ and $\tau_{R\parallel}$. They refer to reorientation of the symmetry axis of the diffusion tensor and to rotation about this axis, respectively.

Correlation times for long-axis fluctuations are difficult to extract from powder averaged T_{1Z} data due to the low relaxation strength of this motion. However, the orientation dependence of the spin–lattice relaxation is found to be sensitive to the rate and amplitude of the wobbling motion. Correlation times for cholesterol fluctuations have thus been determined by analyzing the T_{1Z} anisotropy of cholesterol-3α-d_1 (see Figure 5b). Note that the data were fitted by using only one adjustable parameter, namely, the motional rate of the fluctuation, while all other parameters have reliably been determined from temperature-dependent studies.

In Figure 12 the correlation times $\tau_{R\parallel}$ and $\tau_{R\perp}$ of cholesterol (crosses) are plotted as a function of $1/T$. The uncertainty in both correlation times is generally <20%. Included are corresponding values for the phospholipids (triangles and squares) in the mixed bilayer. The dashed line indicates the main transition of pure DMPC membranes. We see that the Arrhenius plots for cholesterol are linear above 273 K. The evaluated constant anisotropy ratio of $\tau_{R\perp}/\tau_{R\parallel} = 30$ corresponds to theoretical expectations. From the slopes of the straight lines, an activation energy of $E_R = 38$ kJ/mol can be determined (see Table II). This value is comparable to the corresponding activation energy found for DMPC in the same

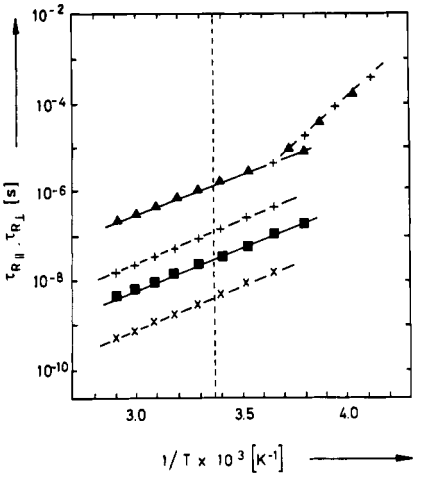

FIGURE 12: Arrhenius plot of the correlation times $\tau_{R\parallel}$ (×) and $\tau_{R\perp}$ (+), characterizing overall rotation and fluctuation of cholesterol in DMPC/cholesterol mixed membranes (40 mol % cholesterol). Also included are the corresponding correlation times $\tau_{R\parallel}$ (■) and $\tau_{R\perp}$ (▲) for DMPC in the mixed bilayers. The dashed line indicates the main transition of pure DMPC membranes.

system and agrees well with the activation energy previously determined by ^{2}H spin–lattice relaxation at different Larmor frequencies (Dufourc & Smith, 1986). Correlation times for axial rotation $\tau_{R\parallel}$ above 273 K are of the order of 10^{-9} s and hence in the most sensitive dynamic range for T_{1Z} relaxation. When compared to the phospholipid, cholesterol rotation is found to be faster by about one order of magnitude, therefore excluding any long-lived cholesterol/phospholipid complex at higher temperatures.

Analysis of the T_{1Z} relaxation curve minimum [$(T_{1Z})_{min}$ = 6 ms], dominated by axial rotation of the steroid, suggests that the quadrupolar interaction is preaveraged by rapid low-amplitude motions. These processes are too fast to contribute to spin–lattice relaxation at 46 MHz. Employing a simple relaxation model, these motions were assigned to long-axis librations of the cholesterol ring system (Dufourc & Smith, 1986). On the basis of our results and former EPR (Kar et al., 1985; Shin & Freed, 1989) and ^{13}C NMR (Brainard & Cordes, 1981; Brainard & Szabo, 1981) investigations, these motions are clearly different from long-axis fluctuations, associated with rotational diffusion of the molecules as a whole.

As was already observed for the phospholipid, the quadrupole echo spectra of cholesterol-3α-d_1 exhibit two components with different intermolecular dynamics over a limited temperature range (273 K < T < 263 K) (see Figure 3b). Below 263 K, only the "immobile" component is left, exhibiting slow fluctuations with correlation times $\tau_{R\perp} > 10^{-6}$ s equal to those found for DMPC. The common T_{2E} course, observed for labeled cholesterol and phospholipid at low temperatures (see Figure 6), argues against separation of cholesterol crystals but rather indicates a similar molecular organization of both lipid components in a homogeneous environment. The increase of the activation energy from 35 to 80 kJ/mol for fluctuations of the "immobilized" sterol reflects the stronger intermolecular interactions in this temperature regime and corresponds to the changes found for DMPC. Interestingly, correlation times for cholesterol long-axis fluctuations are equal to those observed for the phospholipid in this region.

Elastic Modes. So far we have focused on the motions of individual molecules, which fully account for spin–lattice relaxation in the conventional megahertz range. However, the short spin–spin relaxation times, observed above T_M (see Figure 6), cannot be described by fast molecular reorientations with correlation times of 10^{-7} s > τ_R > 10^{-12} s. Rather,

Table III: Parameters Characterizing Collective Lipid Motions in Bilayer Membranes

system	temp T (K)	av elastic const K (N)	effective bilayer viscosity η (P)	long wavelength cutoff λ_l (m)
pure DMPC[a]	318	1×10^{-11}	0.10	3×10^{-6}
pure DMPC[b]	313	1×10^{-11}	0.10	5×10^{-6}
DMPC 40 mol % cholesterol	318	3.5×10^{-11}	0.37	3×10^{-6}

[a] From ^{2}H NMR (this work). [b] From ^{31}P NMR (Dufourc et al., 1992).

low-frequency motions with $\tau_R > 10^{-6}$ s are expected to contribute to the transverse relaxation at higher temperatures. Ample evidence for slow motions to occur in liquid-crystalline membranes comes from spin–lattice relaxation studies in the rotating frame (Cornell & Pope, 1980; Pope et al., 1982; Peng et al., 1989) and at low laboratory fields (Rommel et al., 1988) as well as from measurements of the transverse relaxation in quadrupole echo (Watnick et al., 1987, 1990a; Kothe & Stohrer, 1992) and CPMG pulse sequences (Bloom & Sternin, 1987; Stohrer et al., 1991; Dufourc et al., 1992). Recently, a detailed analysis of the anisotropy and pulse frequency dispersion of ^{2}H spin–spin relaxation rates revealed that order director fluctuations represent a major transverse relaxation process in fluid bilayer membranes (Stohrer et al., 1991).

The relaxation model for these slow collective lipid motions (see Figure 1) predicts the dependence of T_{2E} on the average director orientation to be $T_{2E} \sim (\cos^2 \xi \sin^2 \xi)^{-1}$ (eq 7). We find that T_{2E} of 2-[*6,6-d*$_2$]DMPC in the cholesterol-containing membrane is largest at the $\xi = 0°$ and $\xi = 90°$ orientations, exhibiting the shortest value at $\xi \sim 45°$ (see Figure 7a). Apparently, the observed angular dependence is consistent with order director fluctuations.

Interestingly, for pulse spacings $t_1 > 100$ μs the transverse relaxation times T_{2E}^{CP} from CPMG pulse sequences still exhibit a strong t_1 dependence. This result immediately shows that correlation times longer than 100 μs play an important role in the transverse ^{2}H spin relaxation of DMPC bilayers above T_M (Bloom & Sternin, 1987; Stohrer et al., 1991). Plotting T_{2E}^{CP} as function of the pulse frequency $\omega = 1/t_1$ yields the relaxation dispersion curves shown in Figure 8. The data refer to 2-[*6,6-d*$_2$]DMPC in pure (open symbols) and cholesterol-containing bilayers (filled symbols). Apparently, in both cases there is a broad interval where $T_{2E}^{CP}(\omega)$ is proportional to ω^1. Such a linear frequency dependence is characteristic of *two-dimensional order director fluctuations* (eq 7), which thus constitute the dominant transverse relaxation process above T_M (Stohrer et al., 1991). Analysis of this linear regime [$T_{2E}^{CP}(\omega) \sim \omega^1$] provides reliable values for the average elastic constant K of the membranes (eq 7).

For pulse frequencies $\omega < \omega_l$, where ω_l denotes the low-frequency cutoff of the elastic modes, the dispersion of the transverse relaxation time $T_{2E}^{CP}(\omega)$ should gradually disappear, and in the limit $\omega \rightarrow 0$ we expect $T_{2E}^{CP}(0)$ to be equal to T_{2E}, as observed experimentally (see Figure 8). This finding allows determination of the effective bilayer viscosity η and the long wavelength cutoff λ_l of the elastic modes (eq 8).

Interestingly, adding salt to the sample is found to have significant effects on the transverse ^{2}H spin relaxation but not on the longitudinal relaxation above T_M. Since electrostatic interactions of the charged phospholipid headgroup may alter the viscoelastic properties of the bilayer, changes in slow cooperative fluctuations are likely to occur while motions of individual molecules should not be affected upon salt addition.

Analysis of the ^{2}H spin–spin relaxation measurements was performed using the relaxation model outlined above (see Materials and Methods). Strictly speaking, a Redfield approach (eqs 7 and 8) is generally not appropriate (Stohrer et al., 1991). Optimized parameters characterizing the hydrodynamic modes of the DMPC membranes are summarized in Table III. Except for λ_l, the maximum error for these parameters is ±30%. The bilayer elastic constant of $K = 3.5 \times 10^{-11}$ N, evaluated for the cholesterol-containing system, exceeds that of the pure membrane by nearly a factor of 4. Using a completely different approach, i.e., videomicroscopy of thermally fluctuating DMPC vesicles, Duwe et al. (1990) found a similar large increase of K in the presence of 30 mol % cholesterol. Likewise, the observed increase of the membrane viscosity from $\eta = 0.1$ P in the pure DMPC bilayer (Stohrer et al., 1991; Dufourc et al., 1992) to $\eta = 0.37$ in the cholesterol-containing system is corroborated by an independent study (El-Sayed et al., 1986).

Apparently, cholesterol significantly increases the average elastic constant of the membrane, thus reducing the density of the collective lipid motions in the mixed bilayer. In contrast, peptides (Watnick et al., 1990b; S. Prosser, J. H. Davis, C. Mayer, K. Weisz, and G. Kothe, unpublished results) and proteins (K. Weisz, N. Ryba, D. Marsh, and G. Kothe, unpublished results) seem to exert opposite effects on the membrane elasticity, therefore enhancing the intensity of the order director fluctuations. It thus appears that the viscoelastic properties of the bilayers are characteristically modified by the presence of particular membrane components. At present, one can only speculate on the biological significance of these directed modulations of the membrane elasticity.

Conclusions

The present work provides a comprehensive description of the complex structural and dynamic organization in binary phospholipid/cholesterol membranes as obtained by pulsed dynamic NMR. Cholesterol is found to affect both fast molecular reorientations and slow collective fluctuations of the lipids. While changes in the molecular order and dynamics of individual lipid molecules have long been recognized as an important aspect of cholesterol incorporation, the modulation of long-range cooperative motions has only recently been realized as of importance for many interactions within the membrane. The possibility to quantitatively characterize slow motions makes ^{2}H NMR an ideal technique for further studies of these low-frequency modes in the presence of specific membrane components, essential for a better understanding of their biological significance.

Acknowledgments

We thank Mrs. B. Omiecienski for her chemical expertise in the preparation of specifically deuterated lipids and Dr. E. Ohmes for his assistance in the computations.

Registry No. DMPC, 18194-24-6; cholesterol, 57-88-5.

References

Alecio, M. R., Golan, D. E., Veatch, W. R., & Rando, R. R. (1982) *Proc. Natl. Acad. Sci. U.S.A. 79*, 5171.
Blicharski, J. S. (1986) *Can. J. Phys. 64*, 733.
Bloom, M., & Sternin, E. (1987) *Biochemistry 26*, 2101.
Bloom, M., & Mouritsen, O. G. (1988) *Can. J. Chem. 66*, 706.
Blume, A., & Griffin, R. G. (1982) *Biochemistry 21*, 6230.
Bonmatin, J. M., Smith, I. C. P., & Jarrell, H. C. (1988) *J. Am. Chem. Soc. 110*, 8693.

Bonmatin, J. M., Smith, I. C. P., Jarrell, H. C., & Siminovitch, D. J. (1990) *J. Am. Chem. Soc. 112*, 1697.
Boyanov, A. I., Koynova, R. D., & Tenchov, B. G. (1986) *Chem. Phys. Lipids 39*, 155.
Brainard, J. R., & Cordes, E. H. (1981) *Biochemistry 20*, 4607.
Brainard, J. R., & Szabo, A. (1981) *Biochemistry 20*, 4618.
Brown, M. F. (1990) *Mol. Phys. 71*, 903.
Butler, K. W., Smith, I. C. P., & Schneider, H. (1970) *Biochim. Biophys. Acta 219*, 514.
Cornell, B. A., & Pope, J. M. (1980) *Chem. Phys. Lipids 27*, 151.
Cornell, B. A., Davenport, J. B., & Separovic, F. (1982) *Biochim. Biophys. Acta 689*, 337.
Cornell, B. A., Hiller, R. G., Raison, J., Separovic, F., Smith, R., Vary, J. C., & Morris, C. (1983) *Biochim. Biophys. Acta 732*, 473.
Cotter, M. A. (1977) *J. Chem. Phys. 66*, 1098.
Das Gupta, S. K., Rice, D. M., & Griffin, R. G. (1982) *J. Lipid Res. 23*, 197.
Davies, M. A., Schuster, H. F., Brauner, J. W., & Mendelsohn, R. (1990) *Biochemistry 29*, 1990.
Davis, J. H. (1979) *Biophys. J. 27*, 339.
De Gennes, P. G. (1974) *The Physics of Liquid Crystals*, Clarendon Press, London.
De Kruyff, B., Demel, R. A., & Van Deenen, L. L. M. (1972) *Biochim. Biophys. Acta 255*, 331.
Dufourc, E. J., Parish, E. J., Chitrakorn, S., & Smith, I. C. P. (1984) *Biochemistry 23*, 6062.
Dufourc, E. J., & Smith, I. C. P. (1986) *Chem. Phys. Lipids 41*, 123.
Dufourc, E. J., Mayer, C., Stohrer, J., Althoff, G., & Kothe, G. (1992) *Biophys. J. 67*, 1.
Duwe, H.-P., Kaes, J., & Sackmann, E. (1990) *J. Phys. (Paris) 51*, 945.
El-Sayed, M. Y., Guion, T. A., & Fayer, M. D. (1986) *Biochemistry 25*, 4825.
Estep, T. N., Mountcastle, D. B., Biltonen, R. L., & Thompson, T. E. (1978) *Biochemistry 17*, 1984.
Fahey, P. F., & Webb, W. W. (1978) *Biochemistry 17*, 3046.
Fieser, L. J. (1963) *Organic Syntheses, Collect*, Vol. IV, p 195, Wiley, New York.
Flory, P. J. (1969) *Statistical Mechanics of Chain Molecules*, Interscience, New York.
Gally, H.-U., Seelig, A., & Seelig, J. (1976) *Hoppe-Seyler's Z. Physiol. Chem. 357*, 1447.
Haberkorn, R. A., Griffin, R. G., Meadows, M., & Oldfield, E. (1977) *J. Am. Chem. Soc. 99*, 7353.
Heaton, N. J., Vold, R. R., & Vold, R. L. (1988) *J. Magn. Reson. 77*, 572.
Hui, S. W., & He, N.-B. (1983) *Biochemistry 22*, 1159.
Ipsen, J. H., Karlstrom, G., Mouritsen, O. G., Wennerstrom, H., & Zuckermann, M. H. (1987) *Biochim. Biophys. Acta 905*, 162.
Jarrell, H. C., Jovall, P. A., Giziewicz, J. B., Turner, L. A., & Smith, I. C. P. (1987) *Biochemistry 26*, 1805.
Kar, L., Ney-Igner, E., & Freed, J. H. (1985) *Biophys. J. 48*, 569.
Kawato, S., Kinosita, K., & Ikegami, A. (1978) *Biochemistry 17*, 5026.
Kothe, G., & Stohrer, J. (1992) in *Molecular Dynamics in Liquid Crystals* (Luckhurst, G. R., Ed.) Kluwer Academic *Publishers*, Dordrecht, The Netherlands.
Ladbrooke, B. D., Williams, R. M., & Chapman, D. (1968) *Biochim. Biophys. Acta 150*, 333.
Lafleur, M., Cullis, P. R., & Bloom, M. (1990) *Eur. Biophys. J. 19*, 55.
Luz, Z., & Meiboom, J. (1963) *J. Chem. Phys. 39*, 366.
Mabrey, S., Mateo, P. L., & Sturtevant, J. M. (1978) *Biochemistry 17*, 2464.
Marqusee, J. A., Warner, M., & Dill, K. A. (1984) *J. Chem. Phys. 81*, 6404.
Mayer, C., Müller, K., Weisz, K., & Kothe, G. (1988) *Liq. Cryst. 3*, 797.
Mayer, C., Gröbner, G., Müller, K., Weisz, K., & Kothe, G. (1990) *Chem. Phys. Lett. 165*, 155.
McIntosh, T. J. (1978) *Biochim. Biophys. Acta 513*, 43.
Meier, P., Ohmes, E., Kothe, G., Blume, A., Weidner, J., & Eibl, H.-J. (1983) *J. Phys. Chem. 87*, 4904.
Meier, P., Ohmes, E., & Kothe, G. (1986) *J. Chem. Phys. 85*, 3598.
Moro, G., & Freed, J. H. (1981) *J. Chem. Phys. 74*, 3757.
Müller, K., Meier, P., & Kothe, G. (1985) *Prog. Nucl. Magn. Reson. Spectrosc. 17*, 211.
Needham, D., McIntosh, T. J., & Evans, E. (1988) *Biochemistry 27*, 4668.
Oldfield, E., & Chapman, D. (1971) *Biochem. Biophys. Res. Commun. 43*, 610.
Oldfield, E., Meadows, M., Rice, D., & Jacobs, R. (1978) *Biochemistry 17*, 2727.
Papahadjopoulos, D., Nir, S., & Ohki, S. (1971) *Biochim. Biophys. Acta 266*, 561.
Peng, Z.-Y., Tjandra, N., Simplaceanu, V., & Ho, C. (1989) *Biophys. J. 56*, 877.
Pope, J. M., Walker, L., Cornell, B. A., & Separovic, F. (1982) *Mol. Cryst. Liq. Cryst. 89*, 137.
Presti, F. T., Pace, R. J., & Chan, S. I. (1982) *Biochemistry 21*, 3831.
Redfield, A. G. (1965) *Adv. Magn. Reson. 1*, 1.
Rommel, E., Noack, F., Meier, P., & Kothe, G. (1988) *J. Phys. Chem. 92*, 2981.
Rosenfeld, R. S., Fukushima, D. K., Hellmann, L., & Gallagher, T. F. (1954) *J. Biol. Chem. 211*, 301.
Rubenstein, J. L. R., Smith, B. A., & McConnell, H. M. (1979) *Proc. Natl. Acad. Sci. U.S.A. 76*, 15.
Sankaram, M. B., & Thompson, T. E. (1990) *Biochemistry 29*, 10676.
Schreier-Murillo, S., Marsh, D., Dugas, H., Schneider, H., & Smith, I. C. P. (1973) *Chem. Phys. Lipids 10*, 11.
Seelig, A., & Seelig, J. (1974) *Biochemistry 13*, 4839.
Shimshick, E. J., & McConnell, H. M. (1973) *Biochem. Biophys. Res. Commun. 53*, 446.
Shin, Y.-K., & Freed, J. H. (1989) *Biophys. J. 55*, 537.
Siminovitch, D. J., Ruocco, M. J., Olejniczak, E. T., Das Gupta, S. K., & Griffin, R. G. (1985) *Chem. Phys. Lett. 119*, 251.
Siminovitch, D. J., Ruocco, M. J., Olejniczak, E. T., Das Gupta, S. K., & Griffin, R. G. (1988) *Biophys. J. 54*, 373.
Stockton, G. W., & Smith, I. C. P. (1976) *Chem. Phys. Lipids 17*, 251.
Stohrer, J., Gröbner, G., Reimer, D., Weisz, K., Mayer, C., & Kothe, G. (1991) *J. Chem. Phys. 95*, 672.
Taylor, M. G., & Smith, I. C. P. (1980) *Biochim. Biophys. Acta 599*, 140.
Taylor, M. G., Akiyama, T., & Smith, I. C. P. (1981) *Chem. Phys. Lipids 29*, 327.

Taylor, M. G., Akiyama, T., Saito, H., & Smith, I. C. P. (1982) *Chem. Phys. Lipids 31*, 359.
Thompson, N. L., & Axelrod, D. (1980) *Biochim. Biophys. Acta 597*, 155.
Träuble, H. (1971) *J. Membr. Biol. 4*, 193.
Vist, M. R., & Davis, J. H. (1990) *Biochemistry 29*, 451.
Watnick, P. I., Dea, P., Nayeem, A., & Chan, S. I. (1987) *J. Chem. Phys. 86*, 5789.
Watnick, P. I., Dea, P., & Chan, S. I. (1990a) *Proc. Natl. Acad. Sci. U.S.A. 87*, 2082.
Watnick, P. I., Chan, S. I., & Dea, P. (1990b) *Biochemistry 29*, 6215.

Gramicidin Conformational Studies with Mixed-Chain Unsaturated Phospholipid Bilayer Systems†

Kingsley J. Cox, Cojen Ho, Joseph V. Lombardi, and Christopher D. Stubbs*
Department of Pathology and Cell Biology, Thomas Jefferson University, Philadelphia, Pennsylvania 19107
Received March 18, 1991; Revised Manuscript Received August 27, 1991

ABSTRACT: The transition of gramicidin from a nonchannel to a channel form was investigated using mixed-chain phosphatidylcholine lipid bilayers. Gramicidin and phospholipids were codispersed, after removal of the solvents chloroform/methanol or trifluoroethanol which resulted in nonchannel and channel conformations, respectively, as confirmed using circular dichroism (CD). The fluorescence emission maxima of the nonchannel form were shifted toward shorter wavelengths by heating at 60 °C (for 0–12 h), which converted it to a channel form, again as confirmed by CD. The channel form did not respond to heat treatment. Heat treatment also increased the fluorescence anisotropy of the nonchannel gramicidin tryptophans. The rate of transition from the nonchannel to channel conformation was found to be faster if phosphatidylethanolamine was present in combination with phosphatidylcholine compared to phosphatidylcholine alone. Also, gramicidin in bilayers of the polyunsaturated 1-palmitoyl-2-docosahexaenoylphosphatidylcholine converted more rapidly compared to 1-palmitoyl-2-oleoylphosphatidylcholine. Using the fluorescence anisotropy of the membrane lipid probe 1,6-diphenyl-1,3,5-hexatriene, it was also shown that the motional properties of the surrounding lipid acyl chains differed for the channel and nonchannel gramicidin conformations. The possibility that lipids tending to favor the hexagonal phase (H_{II}) would enhance the rate of the nonchannel to channel transition was supported by ^{31}P NMR which revealed the presence of some H_{II} lipids in the channel preparations. The results of this study suggest that gramicidin may serve as a useful model for similar conformational transitions in other more complex membrane proteins.

Gramicidin is a hydrophobic pentadecapeptide composed of alternating L- and D-amino acids which span the lipid bilayer to form a cation channel in the form of a β6.3 left-handed helical dimer linked at the N-terminals [see reviews by Anderson (1984), Urry (1985), Cornell (1987), and Wallace (1990)]. The structure is stabilized by alternate intra- and intermonomer hydrogen bonds from the amide NH and formyl C=O groups. One motivation for the study of gramicidin is that is can be used as a model to help in the understanding of more complex systems. This applies not only to its function as an ion channel but also as a model for protein/lipid interactions in general.

Gramicidin has two distinct conformational states which were first recognized in organic solvents [see recent review by Wallace et al. (1990)]. In trifluoroethanol and DMSO, gramicidin is in a monomeric β6.3-helical form. By contrast, in ethanol or chloroform/methanol, a double-helical dimer configuration is found. Using circular dichroism (CD)[1] and NMR, it has recently been shown that when gramicidin is added to lipid bilayers, from trifluoroethanol or DMSO, the β6.3 single helical (channel) conformation is maintained in the bilayer, with two monomers joined at the N-termini, at the bilayer center, to form a dimer comprising the channel configuration (LoGrasso et al., 1988; Killian & Urry, 1988; Killian et al., 1988a,b). A nonchannel (double-helical head-to-tail dimer) conformation resulted if the protein was added from a solution of ethanol or chloroform/methanol. The solvent dependence occurs even if the solvent is completely removed prior to dispersing. The solvent-directed conformation in lipid bilayers has also been demonstrated using high-pressure liquid chromatography where the two forms of gramicidin were recovered from lipid bilayers in their monomeric (channel) and dimeric (helical) configurations (Bano et al., 1989, 1991). A solvent-dependent formation of H_{II} lipids with DOPC has also been demonstrated, with the addition of gramicidin (from trifluoroethanol or DMSO) to preformed bilayers inducing the formation of H_{II} lipids, while addition from ethanol maintained the bilayer phase (Tournois et al., 1987). In earlier studies, it was shown that to obtain gramicidin in a channel form it was necessary to heat phospholipid and gramicidin dispersions at elevated temperatures for several hours [see, for

† This work was supported by US Public Health Service Grants AA08022, AA07186, and AA07215 and by a grant from the Alcoholic Beverage Medical Research Foundation. C.H. was supported by NIAAA Training Grant AA07463.
* Address correspondence to this author.

[1] Abbreviations: CD, circular dichroism; DOPC, dioleoylphosphatidylcholine; DPH, 1,6-diphenyl-1,3,5-hexatriene; H_{II}, hexagonal phase; ^{31}P NMR, phosphorus-31 nuclear magnetic resonance; PC, phosphatidylcholine; PDPC, 1-palmitoyl-2-docosahexaenoyl-PC; PE, phosphatidylethanolamine; POPC, 1-palmitoyl-2-oleoyl-PC; POPE, 1-palmitoyl-2-oleoyl-PE.

0006-2960/92/0431-1112$03.00/0